00971

1988/08/00

[redacted]

Trends and Developments (Special Issue)

A Synthesis of Recent Open-Source Data on Chinese Nuclear Test Locations (U)

A Defense S&T Intelligence Periodical

Defense Intelligence Agency

DST-2660P-107-88-SPR-7
August 1988

[redacted]

[redacted]

(Special Issue)

Trends and Developments in Foreign Technology
Weapons and Systems

A Synthesis of Recent Open-Source Data on Chinese Nuclear Test Locations (U)

DST-2660P-107-88-SPR-7

A Defense S&T Intelligence Periodical

Date of Publication: August 1988

This is a Department of Defense Intelligence Document
prepared for the
Directorate of Scientific and Technical Intelligence
by the
Military Geology Project
U.S. Geological Survey
Reston, VA 22092

Author: [redacted]

[redacted]

[redacted]

Introduction (U)

[redacted]

(U) Geophysical data in this area have been sparse and the new, detailed, site-specific data which include longitudinal wave velocities and physical properties, fill a large gap.

[redacted]

(U) In order to determine the effect of a nuclear explosion on the rock velocity, a sampling program was undertaken, starting from a scaled distance of 102 $m/kt^{1/3}$ from the explosion center. A total of 19 sampling points were taken, 32 sample blocks were prepared. The samples were cut to 5.5 cm diameter and 5-9 cm length. Variations were found in the longitudinal wave velocities of the granite samples: at a scaled distance of 11 $m/kt^{1/3}$ from the explosion center the average Vp was 4068 m/sec. Beyond a scaled distance of 38 m/kt^{13} the rock sample velocity is essentially the same as the rock velocity prior to the explosion, averaging 4743 m/sec. The difference between the two average values is about 14%. The graph in Figure 4 shows that the slowest rock samples were taken near the shaft, and the velocity gradually increases with distance from the shaft until it reaches the undisturbed "pre-explosion" velocity value.

(S/NF) Reference 4 (which is found in the same volume and series as Reference 2) discusses a single vertical shaft, "Hole No. 709", (believed to be at Location E, either Chic 24 or Chic 29). The rock from this hole is also described as a biotite plagioclase granite, composed mostly of quartz, feldspar, and biotite. Data presented in the tables accompanying Reference 4 indicate that the shaft is (at least) 304 m (~1000 ft.) deep (see Table IV, Appendix). Apparently pre-existing fractures in the rock are aligned to the northeast and northwest.

(U) Some physical properties of a rock test sample are presented in Table III (see Appendix). In comparing the compressive, tensile, and shear strength values of this table with data elsewhere (Table II) it is evident that the data in Table III correlate to a depth of 117-259 m in hole No. 709. The article states that the upper 50 m of the test hole had well

[redacted]

UNCLASSIFIED

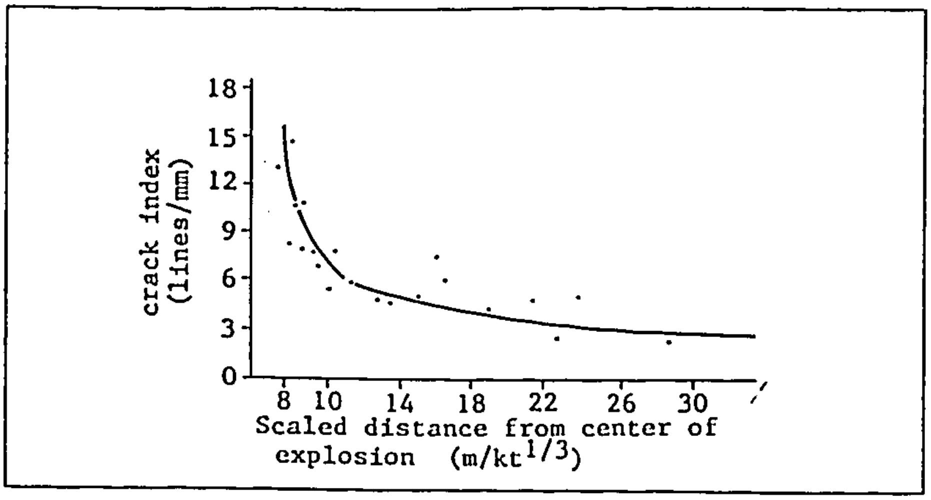

Figure 3 (U). Relationship between the crack index and scaled distance from center of explosion for quartz under effect of shock waves. (From Reference 2, p. 114).

UNCLASSIFIED

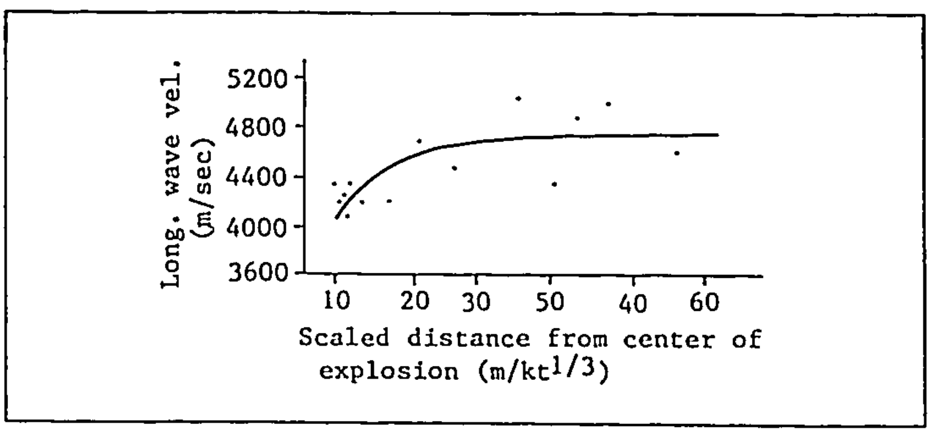

Figure 4 (U). Relationship between longitudinal wave velocity and scaled distance from center of explosion in black mica plagioclase granite. (From Reference 2, p. 112).

[redacted]

developed fractures prior to the explosion, while below 50 m the rock was intact, and that "abnormal" sound velocities, caused by fractures, existed at depths of 130-150 m and at 199 m in the hole. On the basis of established engineering classification standards (Table I, Appendix) and the values of the intact, crack, and weathering coefficients (defined in Table I) obtained for the hole (presented in Table II), the entire rock mass of hole No. 709 was considered to be stable prior to the explosion. The development of a weathered layer and fractures in the upper part of the hole had no apparent effect on rock stability.

(U) The article goes on to state that the "maximum boundary of influence" of the nuclear explosion was 2.5 km from the (projected) center of the explosion, while the maximum boundary of "severe" disturbance was approximately 200 m, and the maximum region of instability was 84 m from the projected explosion center. "The destruction of the surface rock mass was controlled by fault structures;" holes no. 709, 702, 707, and 710 showed dislocations at a depth of 5, 70.13, 10.04, and 17 m respectively, after the explosion. Specific locations of these holes are not identified in the reference.

(U) Post-test investigations showed that the stability of the rock mass was greatly reduced in Hole No. 709. The post-test longitudinal wave velocity, above 60 m depth, was 20% lower than the pre-test wave velocity, while the wave velocity decrease was 43% in between 217-304 m depth. This, and other pre- and post-test comparisons are presented in Figures 5 and 6, below.

[redacted]

UNCLASSIFIED

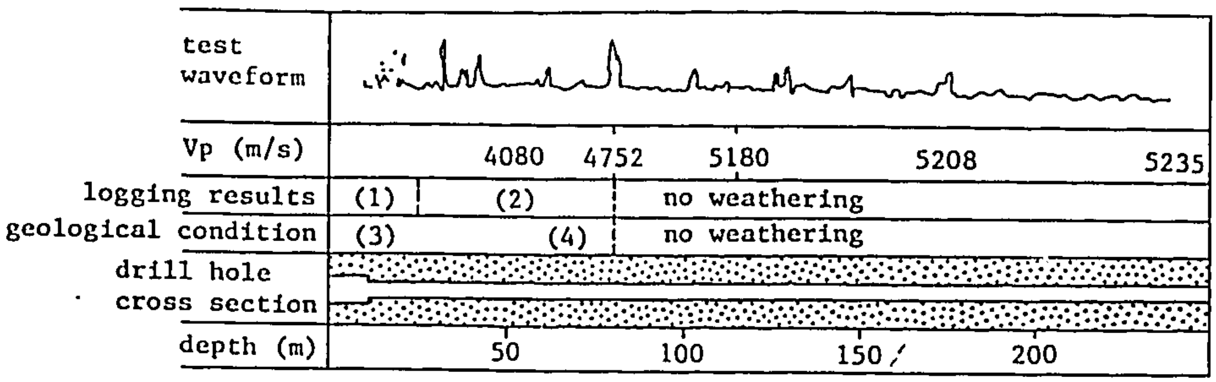

Key: 1. No water
2. Slight to weak weathering
3. Weak weathering
4. Slight weathering

Figure 5 (U). Pre-explosion sound wave test results of black mica plagioclase granite in Hole No. 709. (From Reference 4, p. 119).

UNCLASSIFIED

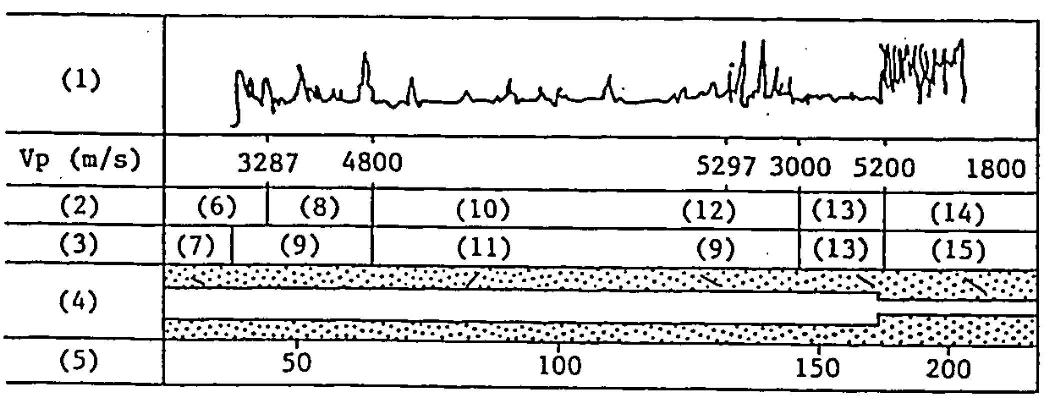

Key:
1. test waveform
2. logging results
3. geological condition
4. drill hole cross section
5. depth (m)
6. severely spalled region
7. no water
8. region affected by spallation
9. rock core fragmented
10. stable region of rock mass
11. rock core intact
12. cracked, loose region
13. steel tubes
14. gravel region
15. rock core extremely fragmented

Figure 6 (U). Post-explosion sound wave logging results of black mica plagioclase granite in Hole No. 709. (From Reference 4, p. 123).

[redacted]

(U) Water leakage into the hole was also a problem. Between 242-279 m steel tubes were used to protect the shaft walls, while below 279 m, cement was injected for protection. In comparing the pre- and post-test data, (Tables II and IV, respectively) it is seen that as the longitudinal wave velocity decreases, the elastic and mechanical parameters of the rock also decrease. The conclusions reached in References 2 and 4 concerning the elastic and mechanical parameters of the rock in Location E are as follows:

1. The sonic velocity drops in the vicinity of the cavity wall.

2. The shock waves from the nuclear explosion cause microcracks in the rock, which in turn cause the sonic velocity to drop.

3. The sonic velocity gradually increases with increasing distance from the explosion center, until it reaches the pre-explosion value beyond a certain distance (about 38 $m/kt^{1/3}$ in Hole No. 709).

4. The originally stable rock mass becomes fragmented and unstable, with well developed fractures, after the explosion.

5. If a stable rock mass of "insufficient" thickness is located between two unstable rock masses, the safety of subsequent tests will be adversely affected.

6. The degree and depth of "spallation" of the land surface are related to the extent of the weathered layer.

7. The existence of a weathered layer reduces the tensile strength of a rock mass.

8. The area of destruction (around hole No. 709) is defined to be between the explosion chamber and a distance of 38 $m/kt^{1/3}$ from the explosion center. This is the region of permanent deformation; the area beyond this range is the elastic region.

9. The longitudinal wave velocity of the undisturbed granite in the area of the vertical shaft averages about 4740 m/sec. Closer to the borehole, the disturbed granite is slower, at about 4070 m/sec.

[redacted]

Ground water (U)

(U) Most of Reference 3 is concerned with ground water at the test site and its reaction to a nuclear explosion. The reference states that there are two water-bearing bodies in the (Location E) test region - a fractured bedrock water-bearing group, and a fault or "intrusive fracture" water bearing zone, both of which are under water table (unconfined) conditions. The ground water, which is replenished by snow melt to the southwest, flows generally N35°-40° E, with a hydraulic slope of 0.9-2%. When the ground water encounters the east-west "pressurized" faults (labelled F2 and F3 in Figure 2) the water table rises and in the low lying areas, can intersect the land surface to form springs, which are the main drains. Holes drilled within the fractured bedrock water-bearing group may see inflow rates of 100 m^3 per day (a "small amount"), while those drilled within the water-bearing fracture zone may see inflows of several hundred cubic meters per day. The ions contained in the ground water are primarily SO_4, Na and Cl, with mineralization of 1 to 5 g/l; the mineralization increases from the southwest to the northeast.

[redacted]

[redacted]

[redacted]

(U) Abrupt rises in the ground water level were recorded in two wells during Explosion I, and six wells during Explosion II, at the zero-hour of the nuclear explosions (see Figure 7). The curves in Figure 7 show that the water level rises quickly but decreases more slowly. The author of Reference 3 suggests that this abrupt rise is caused by elastic compression deformation of the aquifer due to the passage of the shock wave. Since the porosity of the aquifer is low (0.85-2.80% in the sandstone; 0.80 to 2.60% in the granite), the water in the fractures was squeezed out and is seen as a rise in the water level of the observation wells. As the pressure in the explosion cavity is dessiminated quickly, (within less than one minute), the rising water levels also drop quickly. The paper concludes that there are two basic processes of rapid drop and slow recovery of the water level in the observation wells following a nuclear explosion. The first process is the result of the collapse of the explosion-induced cavity, and the second is caused by regional groundwater replenishment; previous observations indicate that re-establishing initial levels may require up to 280 days.

[redacted]

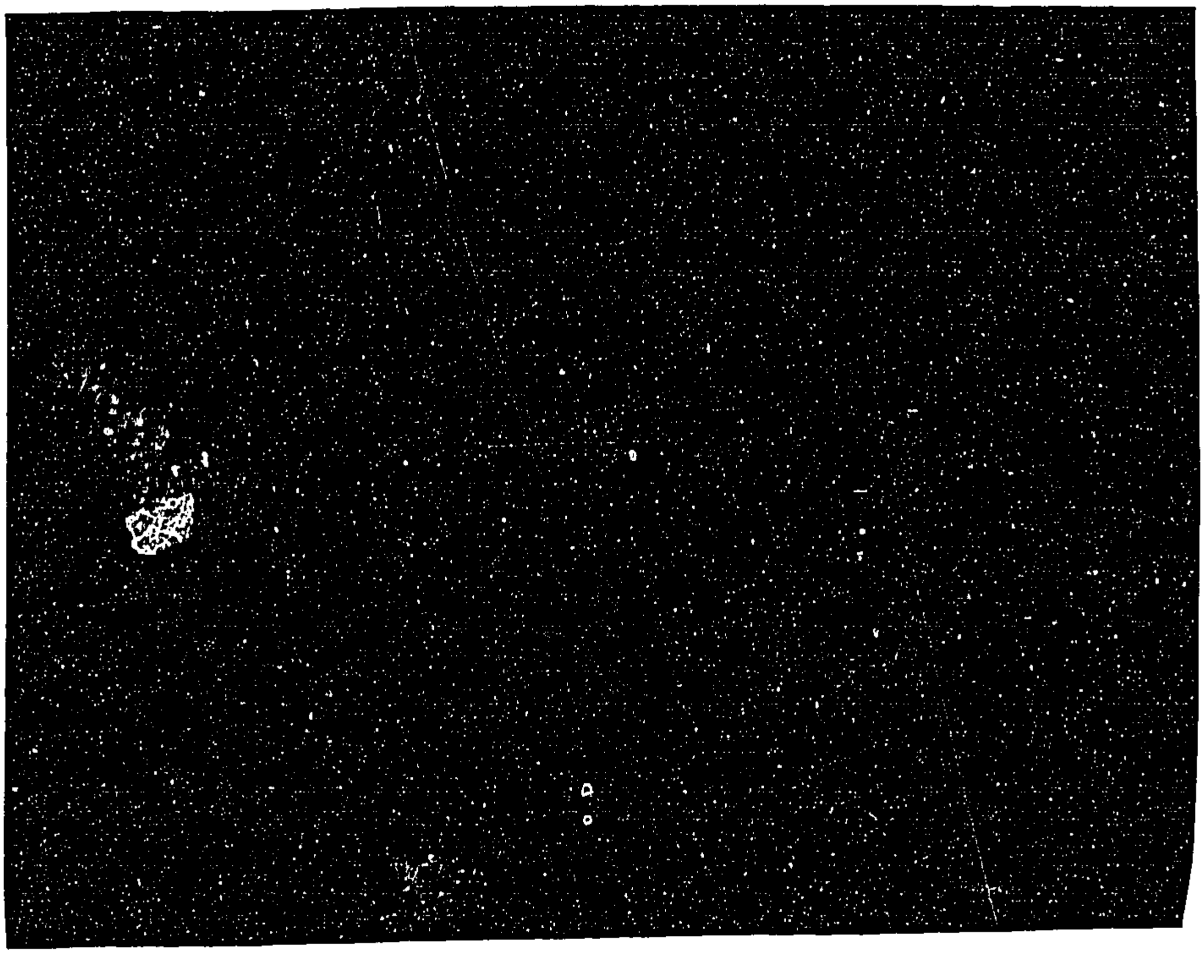

(U) As discussed in Reference 2, rock samples taken close to the cavity wall after a nuclear explosion showed a greater degree of fragmentation than the rock samples taken further away from the shaft. The graph in Figure 3 shows that near the cavity wall, microcracks are 5-6 times more abundant than in the undisturbed rock. Microscopic examination of the rock samples taken near the cavity wall showed that the quartz crystals had been crushed, and microcracks and "knots" had developed in the biotite. All of the rock fragments were less than 5 cm long within a scaled distance of 10.8 $m/kt^{1/3}$ from the explosion center. Beyond a scaled distance of 38-40 $m/kt^{1/3}$ no visible difference in the rock structure was observed.

[redacted]

[redacted]

UNCLASSIFIED

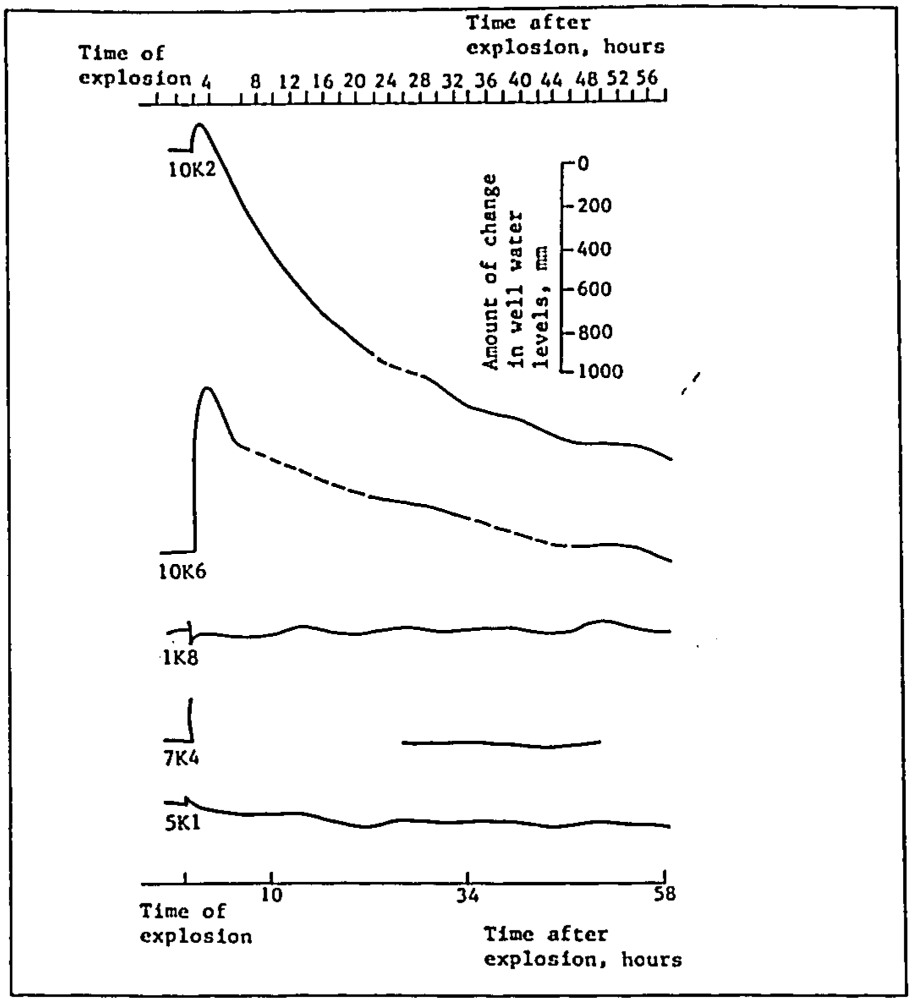

Figure 7 (U). Water level dynamics curves in wells at the time of Explosion II and afterward. (From Reference 3, p. 52).

[redacted]

Horizontal Tunnel (U)
Geology (U)

(U) The geologic environment of a horizontally emplaced nuclear test is described in Reference 2. The rock from a tunnel is described as a "black mica" (biotite) granite, light grayish-red in color, with large crystals and porphyritic texture. The consitituent minerals are: feldspar 60%, and quartz, 30%; plus biotite, amphibole, and pyrite.

[redacted]

[redacted]

[redacted]

UNCLASSIFIED

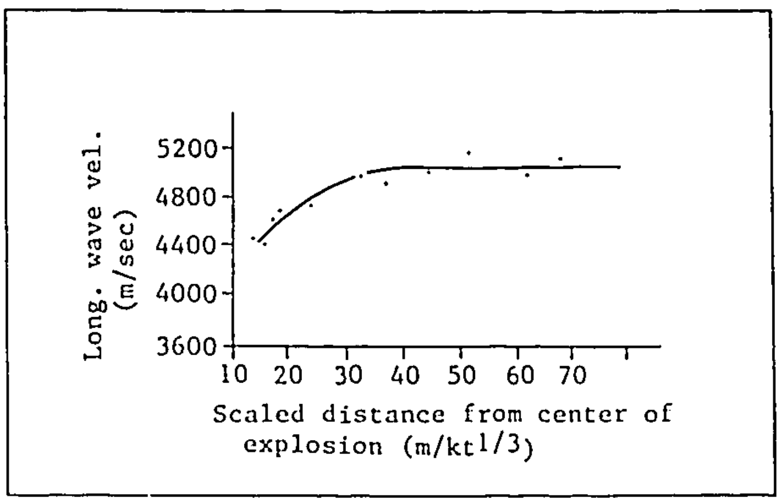

Figure 8 (U). Relationship between longitudinal wave velocity and scaled distance from center of explosion in black mica granite. (From Reference 2. p. 113).

[redacted]

[redacted]

UNCLASSIFIED

TABLE I (U)

Chinese Engineering Classification Standards

	Rock Mass				
	Extremely unstable	Unstable	Poor Stability	Basically Stable	Stable
Intact Coefficient	<0.2	0.2-0.35	0.35-0.5	0.5-0.7	>0.75
Crack Coefficient	>0.8	0.65-0.85	0.5-0.65	0.25-0.5	<0.25
Weathering Coefficient	-	-	-	0.1-0.2	<0.1

Ref.4

UNCLASSIFIED

NOTES:

1. Intact Coefficient = V^2pm/V^2pr , where Vpr = longitudinal wave velocity of test sample
   Vpm = longitudinal wave velocity of the rock mass

2. Crack Coefficient = $\dfrac{(V^2pr - V^2pm)}{V^2pr}$

3. Weathering coefficient = $\dfrac{(Vo - V)}{Vo}$, where Vo = longitudinal velocity of fresh rock
   V = longitudinal velocity of weathered rock

[redacted]

UNCLASSIFIED

TABLE II (U)

Pre-explosion classification of the degree of weathering and description of the rock mass in drill hole No. 709					
Depth of drill hole (M)	26 - 50	50 - 85	85 - 117	117 - 176	176 - 259
Long. wave velocity (m/s)	4080	4752	5108	5208	5295
Weathering coefficient	0.23	0.11	0.04	0.04	0.04
Weathering classification	II	I - 0	0	0	0
Degree of weathering	weak weathering	slight weathering	no weathering	no weathering	no weathering
Description of rock mass	Rock texture unchanged; partial color change in minerals surrounding joint plane; massive rock structure.	Rust appears along joint plane, which decreases with increasing depth; original texture of the rock mass remains unchanged.	Original rock texture preserved; joint plane fresh with no evidence of rust.		
Intact coefficient	0.59	0.80	0.92	0.95	0.99
Crack coefficient	0.41	0.20	0.08	0.05	0.01
Description of rock mass	Developed tensile cracks; weathered products on joint plane, rock interior fresh.	Massive rock structure, rock interior fresh.	Massive rock structure rock hard and fresh	Cracks in certain parts; rock hard and fresh	Massive rock structure, rock hard and fresh
Rock quality	Fair	Good	Good	Good	Good
Evaluation	Basically stable	Stable	Stable	Stable	Stable
Compressive strength* (10^5 Pa)	1048	1412	1634.2	1776.3	1776.3
Tensile strength* (10^5 Pa)	45.1	61.2	70.4	76.5	76.5
Shear strength* (10^5 Pa)	37.2	50.5	58.1	63.1	63.1

*Calculated from elastic wave velocity.

Ref. 4

[redacted]

TABLE III (U)

UNCLASSIFIED

Physical and Mechanical Parameters of the Rock Test Sample

Compressive strength* (10^5 Pa)	Tensile strength* (10^5 Pa)	Shear strength* (10^5 Pa)	Elastic modulus (10^{10}Pa)	Shear modulus (10^{10}Pa)	Poisson ratio	Long. wave vel. (m/s)	Lateral wave vel. (m/s)
1776.3	76.5	63.1	6.76	2.81	0.21	5323	3276

*Note: The rock strengths presented here correlate to a depth of 117-259m in Hole No. 709 (see also Table II).

Ref. 4, p. 119

[redacted]

[redacted]

TABLE IV (U)

Post-Explosion Parameters of Rock Mass in Hole No. 709 (based on sound wave test results of figure 5,6).

Depth of drill hole (m)	28-40	40-60	60-80	80-217	217-242	242-279	279-304
Long. wave velocity (m/s)	3287	4000	4800	5297	3000	5200*	1800
Intact coefficient	0.38	0.56	0.81	0.92	0.31	0.31	0.31
Crack coefficient	0.62	0.44	0.19	0.08	0.68	0.68	0.68
Description of rock mass condition	Tensile cracks developed; rock mass fragmented; low rock core extraction rate	Cracks developed; low core extraction rate	Some cracks; rock core extraction rate increased	Cracks partially developed	Rock mass fragmented; texture loose; evidence of collapsed hole	Rock mass fragmented; texture loose; evidence of collapsed hole	Rock mass extremely fragmented and loose; hole collapsed
Evaluation	Poor stability	Basically stable	Stable	Stable	Unstable	Unstable	Extremely unstable
Compressive strength (10^5 Pa)	667.3	1003.1	1444.4	1776.3	564.2		
Tensile strength (10^5 Pa)	29.2	43.2	62.2	76.5	24.2		
Shear strength (10^5 Pa)	23.9	35.6	51.3	63.1	20.0		

* In this segment, steel tubes were used to protect the shaft wall because of fragmented rock mass and collapsed hole. The sound velocity values listed are measured sound velocities of the steel tubes.

Ref. 4

[redacted]

[redacted]

TABLE V (U)

UNCLASSIFIED

Geologic and Hydrologic Characteristics of Observation Wells
(Locations in Figure 2)

Number	Name of well	Experiment number	Position of Well: Bearing	Position of Well: Distance (km)	Well Structure: Depth of well (m)	Well Structure: Depth of Section (m) / Diameter of well (mm)	Geological Background: Lithology of Aquifer		Geological Background: Structural position of well	Hydrogeological background: Water level (m)	Hydrogeological background: water flow (l/s)	Hydrogeological background: Permeabil (m/day)	Type of Observation Instruments
1	12K2	II	NW276	0.65	151.60	0 a few 151 130 | 110 |	fine sandstone	D_3^4	240 meters from fault	7.95			Kongqi (Red flag)-1
2	10K2	II	SE148	2.17	400.14	0 165 400 130 | 110 |	sandy conglomerate	D_3^4	At the tip of a small fault	8.30	0.0098	0.014	HCJ-1
3	10K5	II	SE148	2.17	829.85	0 a few 830 91 | 78 |	sandy conglomerate	D_3^4	At the tip of a small fault	8.44			SWG-1
4	10K6	II	SE148	2.17	400.63	0 180 401 130 | 110 |	sandy conglomerate	D_3^4	At the tip of a small fault	8.06			HCJ-1
5	1K8	I	NE28	0.72	292.50	0 105 220 292	sandstone & conglomerate	D_3^4	100 meters from intrusion zone	2.95	0.3567	0.088	SZ-1
		II	SW181	2.53	205.30	150 | 120 | 110				3.34			SW-20
6	7K4	I	NW285	1.1	247.00	0 85 247	granite	γ_4^2	400 m from intrusion contact zone	14.90	0.0051	0.015	SSJ-1
		II	SW205	3.4	241.00	150 | 130 |			&150 m from the tip of small fault	14.75			SW-40
7	5K1	II	SW194	4.77	501.00	| |	granite	γ[illegible]	260 m from F_2	33.75	0.0095	0.037	SW-40
8	J13	I	SE179	3.6	347.00	0 150 329 347 150 | 130 | 110	sandstone and quartzite	D_2^4	Axis of an anticline	23.60			Kongqi (Red flag)-1
9	J4	I	NW278	10.5	7.00	0 10 150 | .. |	granite	γ_4^2	50 m from an intrusion contact zone	5.75		0.0085	SW-40
10	J3	I	NW287	12.5	357.00	0 143 291 [illegible]57 160 | 130 | 119	sandstone	D_3^4		28.00	0.0107	0.007	Kongqi (Red flag)-1

Ref. 3, p. 50

[redacted]